

Ising ferromagnets in Ising-percolation square lattices, an example of Ising-Ising coupling

J. Cheraghizadeh* and M. N. Najafi†

Department of Physics, University of Mohaghegh Ardabili, P.O. Box 179, Ardabil, Iran



(Received 3 September 2018; published 26 November 2018)

In this paper we consider the Ising model (called the dynamical Ising model with dynamical temperature T) on the Ising-correlated percolation lattice. To construct this lattice, another Ising model (which is called the quenched Ising model with quench artificial temperature T_q) is employed to model the correlations between imperfections. We argue that for each quenched temperature, there is a particular dynamical temperature $T_c(T_q)$ for which the dynamical Ising model becomes critical. We present some finite-size arguments (based on the moments of the magnetism and the energy as well as the spanning cluster probability) to extract the critical points and also show that they are compatible with the finite-size scaling of the singular point of the magnetic susceptibility. The model is thoroughly characterized in and out of these points. We find that the critical behaviors of the model change significantly with respect to the regular Ising model as well as the Ising model on the uncorrelated percolation lattice. It is shown that for the critical lattice, $T_q = T_c^{\text{square Ising model}} \approx 2.269$, the critical temperature for the dynamical Ising model in the thermodynamic limit is $T_c(T_q = T_c^{\text{square Ising model}}) = 1.94 \pm 0.005$, and the fractal dimension of the exterior perimeter of geometrical spin clusters is $D_f^{T=T_c(T_q=2.269)} = 1.408 \pm 0.002$. Many quantities, such as the dynamical critical temperatures, all local and global critical exponents, and the fractal dimension of loops D_f , scale with the quench temperature in a power-law fashion, with some critical exponents that are reported. Significantly we see that $D_f^{T=T_c(T_q)} - D_f^{T=T_c(T_q=2.269)} \sim \frac{1}{\sqrt{\zeta(T_q)}}$ in which $\zeta(T_q)$ is the correlation length of the quenched Ising model at temperature T_q .

DOI: [10.1103/PhysRevE.98.052136](https://doi.org/10.1103/PhysRevE.98.052136)

I. INTRODUCTION

There are many reasons to consider the magnetic models on imperfect host systems which realize the porous media. This is mainly motivated by some experiments in which the voids of percolating clusters were filled by (commonly magnetite) nanoparticles of a ferromagnetic fluid [1–7]. On the other hand the notion of a critical phenomenon on the fractal lattices [8,9] has attracted much attention, e.g., the sandpiles on uncorrelated [10,11] and correlated [12] host media, random walks on the systems with imperfections [13,14], and mixing of statistical models [15]. It is known that the properties of the statistical critical models on the fractal lattices are tuned by the details of the topological quantities of the fractal lattice, mainly the cluster fractal dimension, the order of ramification, and the connectivity [16], and no lower critical dimension can be defined for them. The Ising model as a simple binary magnetic model has been considered on the uncorrelated percolation lattices, which is a simple realization of the porous media without correlation between the configuration of imperfections [17]. The host media are therefore tuned by the percolation threshold p in that model, which along with the temperature T presents a complete description of the model. We have two order parameters in such a study: the spanning cluster probability [SCP(T, p)], which is defined as the probability that a random chosen site belongs to a spanning geometrical spin cluster (a cluster of connected

parallel spins which connects two opposite boundaries of the system), and the magnetization $M(T, p)$. Two phase transitions for these systems are present: the percolation transition (occurring at $T = T_p$) in which the value of SCP drops from zero (nonpercolating phase) to nonzero values (percolating phase) and the magnetic transition (occurring at $T = T_M$) at which M changes from zero values (paramagnetic phase) to nonzero values (ferromagnetic phase). These transitions are not necessarily simultaneous.

For modeling the stochasticity in the host media, one can use annealed bond or site dilution and quenched dilutions. The former is more tractable analytically (in terms of generalized q -state Potts model), and the latter is more realistic. The Ising q -state Potts model can simultaneously take bond dilution and Ising dynamics into account, i.e., the $q \rightarrow 1$ limit coincides with the Ising model on the annealed percolation lattice [18] in which q controls the number of clusters in the system. It was shown in this model that the lines of the percolation and the magnetic transitions occur in some distinct regions depending on the value of q and there are some multicritical points. The interesting feature of this study is that the transition of the nonpercolating-paramagnetic (NP) phase to percolating-ferromagnetic (PF) phase is first order, whereas the percolating-paramagnetic (PP) to percolating-ferromagnetic (PF) and also the NP to percolating-paramagnetic (PP) phases are second-order transitions, and the position of multicritical points were calculated [18].

The quenched disorder is, however, more challenging, for which many results are available. According to the Harris criterion the relevance or irrelevance of the disorder depends

*jafarcheraghizadeh@gmail.com

†morteza.nattagh@gmail.com

on the α exponent, which is the critical exponent of the specific heat, i.e., only for the case $\alpha > 0$ will the disorder change the critical behaviors. For the Ising model, however, $\alpha = 0$ (it is marginal), which makes the problem worthy to study more deeply. It was shown that the magnetic critical temperature T_c linearly increases with p , and near $p = p_c$ the peak of c_v becomes smoother [19]. The smoothing of c_v is an expected result for this problem. Many works focused on the problem, and many different opinions emerged. One of the primary works has been done by McCoy *et al.* [20], and generalized by Shankar *et al.* [21], in which it was shown that for the Ising model with randomly varying vertical bond the critical behaviors are thoroughly modified, e.g., the specific heat does not diverge, in agreement with some experiments [22,23]. Their model was not, however, clearly related to the real problem since it really concerns the one-dimensional distribution of the disorder. In a very different treatment it was argued that the effect of impurities in a two-dimensional (2D) bond-diluted Ising model is to add a four-fermion interaction with the corresponding charge proportional to the concentration of impurities [24], whose prediction was that for the weak disorder exponent of the spin-spin correlation function η is zero, and that the specific heat is divergent with the logarithmic corrections, i.e., $C_v \sim t^{-\alpha} \ln \ln(\frac{1}{t})$, for which $\alpha = 0$ and $t = (T - T_c)/T_c$. Ludwig [25], however, predicted that $\eta = \frac{1}{4}$ just like in the pure Ising case. These results were confirmed and generalized later [26] and revealed that the critical behaviors should be corrected by logarithmic expressions (see Ref. [17]). Also the 2D Ising model in which bonds fluctuate randomly about a threshold was considered in Ref. [27], in which it was exactly shown that the two-point function behaves like $(\ln R)^{1/4} R^{-1/2}$ with distance R at the critical point. These results have been argued by some other authors analytically [28–30] and numerically [31–34]. The field seems to be active, and the problem is open yet.

Despite this huge literature, little attention has been paid to the effect of configurational pattern of voids of the host media and the correlations between these imperfections. Generally the effect of such correlations is considerable for the systems in the critical region [15,35,36]. In the present paper we aim to measure the effect of the correlations of the spatial configuration of the imperfections of the porous media. To this end, we employ the Ising model (not to be confused with the dynamical Ising model which is supposed to be defined on the lattice). We consider an *artificial temperature* of this Ising model, namely, T_q (in which “ q ” stands for *quench*), which tunes the correlations. To be distinguishable, we show the temperature of the dynamical Ising model by T . We emphasize that the dynamical model with real temperature T and the quenched Ising model (QIM) (that is employed to model the imperfection pattern of the host media) with the artificial temperature T_q should not be confused. Using the QIM, we prepare a (correlated) percolation lattice upon which the dynamical model is defined. In this problem we have two kinds of averaging: one over real (dynamical) Ising samples and over quenched Ising-percolation lattices. By this method we introduce correlations into the diluteness pattern in the host media and show that it causes some considerable differences with respect to the case in which the uncorrelated percolation lattice is considered. There are many ways to

insert correlations into an uncorrelated percolation lattice. These correlations can be directly introduced by an anomalous scaling factor in the Fourier component of the uncorrelated random landscape [37,38] or by defining a dynamical two-state model to capture the diluteness pattern [39–41]. The latter case, in which the strength and the range of correlations are tuned by temperature, covers many phenomena ranging from the porous media [12] to polymer gelation [40]. The case of study in the present paper concerns with the second one, the Ising model on the QIM lattice. In the artificial QIM, the spins play the role of the *field of the active and inactive sites* over the lattice. We characterize the model in terms of the dynamical temperature T and the temperature of QIM T_q (which we call the *quench temperature* for short). The dynamical critical temperatures are extracted by some detailed finite-size analysis, including the moments of magnetism and energy, and also the spanning cluster probability (SCP). We will see some new critical regimes with critical exponents that are very different from the ones for the regular Ising model [42] and the Ising model on the uncorrelated percolation lattice [17]. The paper has two numerical parts: one about the critical lattice $T_q = T_c^{\text{square Ising model}} \approx 2.269$ (we note that the critical temperature for the Ising model on the square lattice is $T_c^{\text{square Ising model}} \approx 2.269$) and one about off-critical lattices. In the latter case, in the vicinity of the critical quench temperature, some power-law behaviors are seen with critical exponents which are reported in the text. Most importantly the fractal dimension of the perimeter of the geometrical spin clusters D_f scales with T_q in a power-law form with a critical exponent close to $\frac{1}{2}$.

II. THE DEFINITION OF THE PROBLEM AND MAIN RESULTS

In this section we introduce the problem of the present paper: the Ising model on the 2D quenched Ising-percolated lattice. The former is controlled by the real temperature T , and the latter by the artificial temperature T_q , which we call the quenched temperature.

A. The Ising model on the Ising lattice

The magnetic properties of the particles in the porous media is a worthwhile problem to be addressed in the statistical physics. In modeling such porous media, introducing correlations in the spatial activity configuration of the corresponding lattice seems to be reasonable since it is no guarantee that in their growth or fabrication the pores are completely independent, i.e., they have degrees of configurational correlations. Therefore, realizing them with an uncorrelated percolation model seems to be a crude approximation. This motivates one to implement the dynamical models (here the Ising model) on the correlated percolation lattice, in which correlations are controllable. Therefore, we need a binary (which realizes presence or absence of the active site) tunable model. The Ising model is a good candidate for this purpose, since it deals with *artificial spins* (σ), and the correlations are tuned by an artificial temperature (T_q). Here the spins play the role of the field of activity-inactivity (diluteness pattern) of the media. We consider the majority spin sites as the active sites. The

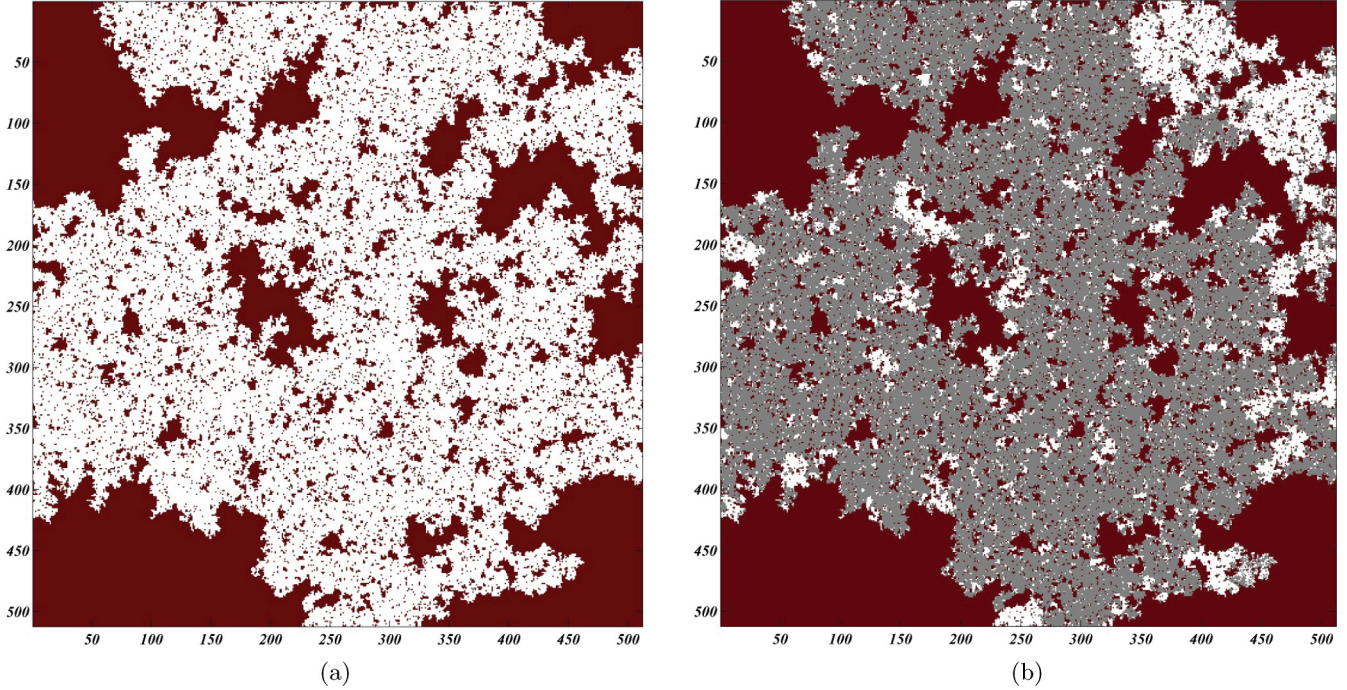


FIG. 1. (a) A 512×512 Ising HSC at $T_q = 2.269$ and (b) a dynamical Ising sample on it with $T = T_c(T_q = T_c)$.

real spins of the dynamical Ising model (s) live in the active sites and interact with the real spins over the active area. The active area is the set of sites which are active. We consider only the host spanning cluster (HSC) from all possibilities and distribute the real spins over these sites (which are involved in the spanning cluster). The HSC is the set of connected active sites which connects two opposite boundaries. Therefore, the dynamics is only on the active ($\sigma = +1$) sites in the HSC. We fix the convention that real spins (for the dynamical Ising system) are shown by s , and artificial spins (for the QIM system) are shown by σ . It is notable that the activity configuration of the media is quenched, i.e., when a quenched Ising configuration is obtained, dynamical Ising samples are generated in the resulting dilute lattice.

Here $\sigma = +1$ ($\sigma = -1$) is attributed to the active (inactive) sites; the QIM Hamiltonian is defined by

$$H = -\frac{1}{T_q} \sum_{\langle i,j \rangle} \sigma_i \sigma_j, \quad \sigma_i = \pm 1, \quad (1)$$

and the dynamical Ising model is defined by

$$H = -\frac{1}{T} \sum_{\langle i,j \rangle} s_i s_j, \quad s_i = \pm 1, \quad (2)$$

both of which are in the zero magnetic field limit [note that the magnetic field in Eq. (1) means the tendency of the system to have more active or inactive sites, which is imposed by external conditions]. $\langle i, j \rangle$ shows that the sites i and j are nearest neighbors. Both models have been considered to be ferromagnetic. The *ferromagnetism* in the QIM (host media) translates to the positively correlated active sites. The artificial temperature T_q , in addition to being the control parameter of the correlations, also controls also the population of the active sites to the total number of sites. This population can also be directly controlled by the *artificial magnetic field*

h_q (zero here), which determines the preferred direction of the quenched spins in the Ising model. For a zero magnetic field ($h = 0$ for the dynamical Ising model and $h_q = 0$ for the QIM) the (dynamical or quenched) Ising model is well known to exhibit a nonzero magnetization per site ($M = \langle s_i \rangle$ for the dynamical Ising model and $M_q = \langle \sigma_i \rangle$ for the QIM) at temperatures below the critical temperature T_c , which is approximately 2.269 in the square lattice. In addition to this transition, a geometrical transition also occurs in which a spanning cluster appears. The probability that a randomly chosen site belongs to a spanning cluster is shown simply by SCP for the dynamical Ising model and by HSCP for the QIM. Apparently SCP (as well as the other exponents of the dynamical Ising model) depends on the artificial temperature T_q . For the regular Ising model (equivalently $T_q \rightarrow 0$) the magnetic and percolation transitions occur simultaneously [43]. We define the Ising model on the $L \times L$ square lattice. First, we need HSC samples, which are obtained by simulating the Eq. (1) at a temperature $T_q \leq T_c$. Then by simulating Eq. (2) on these SCHs at temperature T , some samples are generated to be analyzed locally and geometrically. This is shown in Figs. 1(a) and 1(b), in which the former shows an SCH at $T_q \approx T_c$, and the latter shows a dynamical Ising sample at the critical temperature for the mentioned quenched temperature, $T = T_c(T_q \approx T_c) \approx 1.944$ (this means the critical dynamical temperature for $T_q = T_c \approx 2.269$, which is shown to be around 1.944).

B. Numerical details

We have used the Wolff Monte Carlo method to simulate the system in the vicinity of the critical point to avoid the problem of critical slowing down. Our ensemble averaging contains both averaging over dynamical Ising samples as well

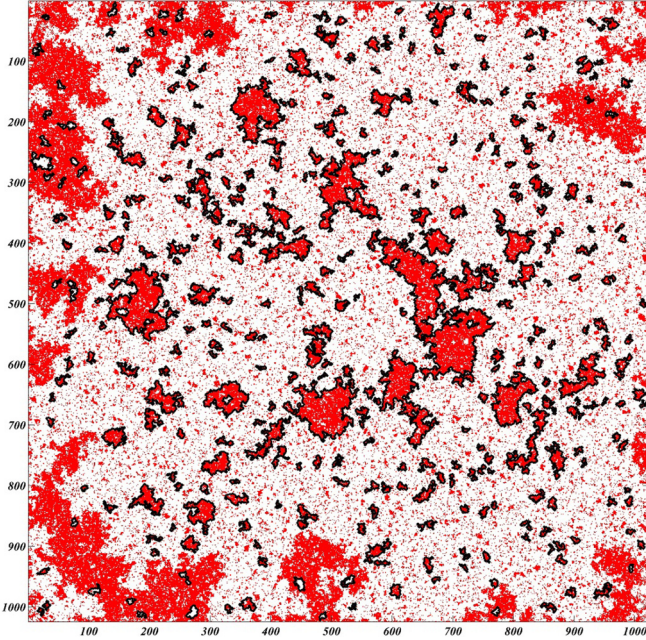


FIG. 2. Loop samples with their corresponding Ising sample media in a 1024×1024 lattice at $T = T_c(T_q \simeq 0)$. The red sites are spin-up and the white sites are spin-down sites. The boundaries of these sites are shown by solid lines.

as HSC averaging. For the latter case we have generated 2×10^3 Ising uncorrelated samples for each temperature on the lattice sizes $L = 128, 256, 512,$ and 1024 . To make the Ising samples uncorrelated, between each successive sampling, we have implied $L^2/3$ random spin flips and let the sample equilibrate with $500L^2$ Monte Carlo steps. The main lattice has been chosen to be square (for which the Ising critical temperature is $T_c \approx 2.269$). Only the samples with temperatures $T \leq T_c$ have been generated, since the HSCs are present only for this case. As stated in the previous section the dynamical spins are put only on the HSCs. The temperatures considered in this paper are T_q and $T = T_c - \delta t_1 \times i$ ($i = 1, 2, \dots, 5$ and $\delta t_1 = 0.01$) to obtain the statistics in the close vicinity of the critical temperature $T_c \simeq 2.269$, and T_q and $T = T_c - \delta t_2 \times i$ ($i = 1, 2, \dots, 10$ and $\delta t_2 = 0.05$) for the more distant temperatures. To equilibrate the Ising sample and obtain the desired samples we have started from the high temperatures ($T > T_c$). For each T and T_q 2×10^3 dynamical Ising samples were generated. An important part of the paper is the geometrical analysis. For identifying the clusters and their boundaries we have used the Hoshen-Kopelman

algorithm. For details see Ref. [44]. Figures 1(a) and 1(b) show a HSC sample and a dynamical Ising sample on it. In the latter the gray area shows the majority spins which are analyzed in this paper. Also Fig. 2 shows a 1024×1024 dynamical Ising sample at $T = T_c(T_q \approx 0)$ with the corresponding external perimeter, which are non-self-intersecting. In our geometrical analysis, along with analyzing the cluster mass (m which is the number of majority spins involved in the cluster), we analyze the gyration radius (r) as well as the length of loops (l). The fractal dimension is defined as the scaling exponent between l and r : $\langle \log l \rangle = D_F \langle \log r \rangle$. Also the distribution function of these quantities is expected to behave like $p(x) \sim x^{-\tau_x}$ in the thermodynamic limit, in which $x = m, l, r$. In the critical state one expects a power-law behavior for the local and geometrical quantities. For example, consider the Bak-Tang-Weisenfeld (BTW) model of sandpiles, for which the distribution functions behave like $p(x) \sim x^{-\tau_x}$ ($x =$ the statistical quantities the system, which are m, l, r here). However, for the finite-size scaling systems there is a region in which the system deviates from power-law behavior, and the distribution functions with respect to some scaling behaviors, named finite-size scaling relations $p_x(x, L) = L^{-\beta_x} g_x(xL^{-\nu_x})$ in which g is a universal function and β_x and ν_x are the exponents corresponding to x . We have extracted τ_x for the largest L in our analysis, $L = 1024$.

C. Main results

For the characterization of the critical properties of the model we first need to find the critical points with controlling the finite-size effects. We argue that for each quench temperature T_q , there is a dynamical temperature $T_c(T_q)$ that the model becomes critical. We present finite-size arguments (on the moments of magnetism and energy as well as the spanning cluster probability to be defined later) to extract the critical points and show that they are compatible with the finite-size scaling of the singular point of the magnetic susceptibility. The model is thoroughly characterized in and out of these critical points. We find that the critical behaviors of the model (at the critical points and in the vicinity of them) significantly change with respect to the Ising model on the regular lattices as well as the uncorrelated percolation lattice. We analyze carefully the critical quenched Ising-correlated lattices, i.e., the lattice for which the quench temperature is critical ($T_q = T_c \approx 2.269$). In this case HSC is itself critical and consequently self-similar with power-law correlations. In this case the effective dimension of the system is $\bar{d} = \frac{187}{96} \simeq 1.948$ [45]. We show that for this case the critical dynamical temperature

TABLE I. The exponents of the model on the critical Ising lattice: $T_q = T_c = 2.269$. For comparison, the third and fourth rows are for the Ising on the uncorrelated percolation lattice [17] and the regular lattice [42], respectively. The generalization of $\tau_l = \frac{d}{D_f} + 1$ [46] to $\tau_l = \frac{\bar{d}}{D_f} + 1$ (in which the effective dimension of the critical Ising model is $\bar{d} = \frac{187}{96}$ [45]) yields 2.4 ± 0.002 , which is consistent with our numerical result.

Model	T_c	β	D_f	γ_{mr}	τ_r	τ_m	τ_l
Ising-Ising	1.944 ± 0.005	0.38 ± 0.01	1.408 ± 0.002	1.981 ± 0.003	3.12 ± 0.03	2.00 ± 0.02	2.45 ± 0.02
Ising percolation	2.93 ± 0.03	–	1.44 ± 0.02	–	2.5 ± 0.2	2.0 ± 0.2	1.9 ± 0.02
Regular Ising	2.269	–	$\frac{11}{8} = 1.375$	–	3.4 ± 0.1	2.31 ± 0.1	2.7 ± 0.1

(i.e., for the dynamical Ising model) in the thermodynamic limit is $T_c(T_q = T_c^{\text{square Ising model}}) = 1.94 \pm 0.005$. Also this temperature varies with quenched temperature in a power-law fashion, i.e., $T_c(T_q) - T_c(T_q = 2.269) \sim (2.269 - T_q)^{\gamma_{TT}}$ in which $\gamma_{TT} \equiv \xi = 0.49 \pm 0.01$. The scaling between l and r (with the exponent γ_{lr} , which is the fractal dimension of the loops) has been analyzed in this work for all temperatures $T \leq T_c$. The other important quantity is the exponent of the magnetic susceptibility ($\chi(T, T_q) \sim |T = T_q|^{\gamma(T_q)}$), for which $\gamma(T_q)$ itself varies with T_q in a power-law fashion with an exponent: $|\gamma(T_q) - \gamma(T_c)| \sim |T - T_q|^\beta$. The fractal dimension of these functions, along with the geometrical spin clusters, the exponents of the distribution function of the gyration radius [$p(r) \sim r^{-\tau_r}$], the cluster mass [$p(m) \sim r^{-\tau_m}$], and the loops' length [$p(l) \sim r^{-\tau_l}$] at $T_q = T_c = 2.269$, have been gathered in Table I.

The other part of the paper concerns the off-critical T_q 's. Importantly, some power-law behaviors have been seen for the off-critical case (but in the vicinity of the critical HSCs), i.e., for the critical dynamical temperatures $T = T_c(T_q)$ with

TABLE II. The secondary spectrum of the (off-critical) exponents of the problem, with their definitions, and the suggested fractional value. $t_q \equiv \frac{T_q - T_c^{2D \text{ square Ising}}}{T_c^{2D \text{ square Ising}}}$.

Exponent	Definition	Value
γ_{TT}	$T_c(T_q) - T_c(T_q = 2.269) \sim t_q^{\gamma_{TT}}$	0.49 ± 0.01
η_{lr}	$D_f(T_c(T_q)) - D_f(T_c(T_q = 2.269)) \sim t_q^{\eta_{lr}}$	0.54 ± 0.04
η_r	$\tau_r(T_c(T_q)) - \tau_r(T_c(T_q = 2.269)) \sim t_q^{\eta_r}$	0.53 ± 0.03
η_l	$\tau_l(T_c(T_q)) - \tau_l(T_c(T_q = 2.269)) \sim t_q^{\eta_l}$	0.52 ± 0.04
η_m	$\tau_m(T_c(T_q)) - \tau_m(T_c(T_q = 2.269)) \sim t_q^{\eta_m}$	0.51 ± 0.02

$T_q \lesssim T_c = 2.269$. These power-law behaviors define some exponents: η_{lr} , η_r , η_l , and η_m . The definition of these exponents is given in Table II, most of which are close to $\frac{1}{2}$. Most importantly one is the fractal dimension, which behaves like

$$D_F(T = T_c(T_q = 2.269)) - D_F(T = T_c(T_q)) \sim \zeta(T_q)^{-\eta_{lr}} \quad (3)$$

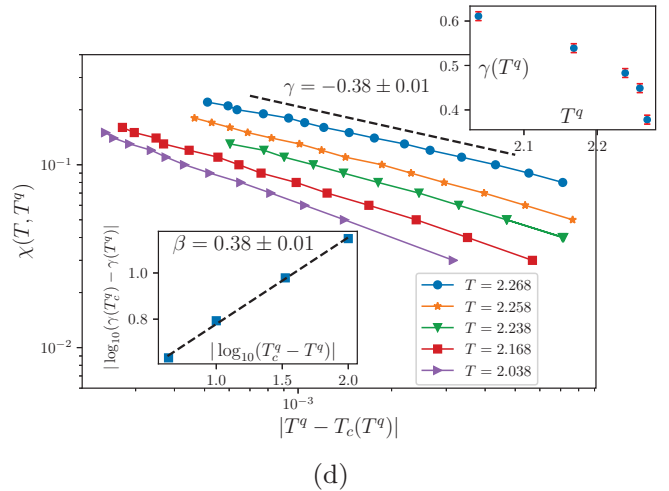
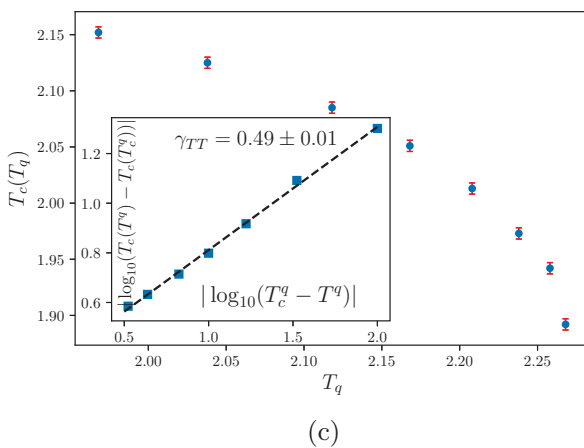
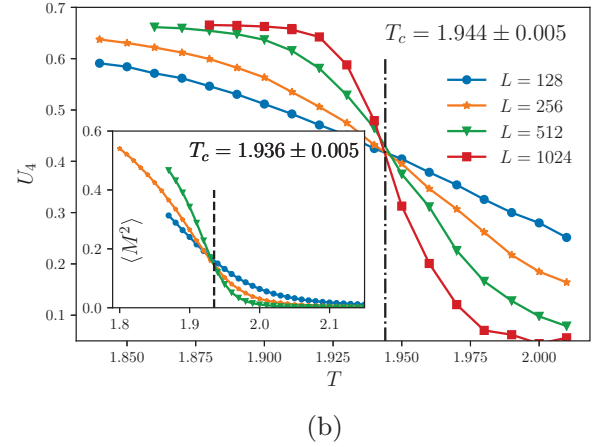
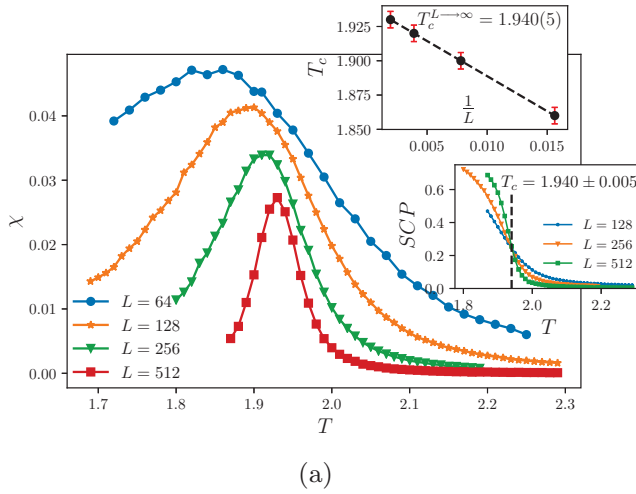


FIG. 3. (a) The magnetic acceptability (χ) in terms of T for various system sizes at $T_q = 2.258$. Upper inset: The position of the peak in terms of $\frac{1}{L}$. Lower inset: The SCP in terms of T for various rates of system size. (b) U_4 (the fourth moment of energy) and $\langle M^2 \rangle$ (the second moment of magnetism) in terms of T for $T_q = 2.258$ and various system sizes. (c) The power-law behavior of the dynamical critical temperature in terms of the quenched temperature T_q . (d) The power-law behavior of magnetic susceptibility $\chi(T, T_q)$. This function behaves in power-law fashion for all considered T_q 's with a varying exponent $\gamma(T_q)$. This dependence is power-law with the exponent β .

with $D_F(T = T_c(T_q = 2.269)) = 1.408 \pm 0.002$ and $\eta_{lr} = 0.54 \pm 0.04$ in which $\zeta(T_q)$ is the spin correlation length of the HSC at the quenched temperature T_q for $L = 1024$.

III. RESULTS

In this section we present the results in more detail. As stated above, we present our results in two subsections: the critical quenched temperature $T_q = T_c \approx 2.269$ and the off-critical HSC with $T_q < T_c$.

Note also that above the T_c the Ising samples do not show percolation. Therefore, since we want to simulate the dynamical Ising model only on the spanning clusters, we do not consider $T_q \leq T_c$. For $T > T_c$ the thermodynamic limit does not exist, i.e., under coarse graining of the system the subcritical islands will disappear.

A. $T_q = T_c^{\text{square Ising model}}$

An accurate determination of the critical dynamical temperature $T_c(T_q)$ for each T_q is required to have a true scaling arguments and estimations for the exponents. We have used four parallel methods to extract $T_c(T_q)$: the singularity of the magnetic susceptibility χ , the finite-size percolation transition points for SCP, the finite-size magnetic transition point for U_4 (which is the fourth moment of the energy), and the second moment of magnetization $\langle M^2 \rangle$. These quantities are shown in Figs. 3(a) and 3(b) for $T_q = T_c = 2.269$. The finite-size analysis of χ shows [upper inset of Fig. 3(a)] that as $L \rightarrow \infty$, $T_c \rightarrow 1.94 \pm 0.05$, which is completely in agreement with the lower inset for SCP. This shows that magnetic and percolation transitions occur simultaneously in $T_q = T_c$. Actually we have examined this for all temperatures and observed that it is the case for all T_q 's. In Fig 3(b) the same results have been obtained based on the analysis of the moments, showing that the curves coincide in a critical point, just the same point of χ divergence: $T_c(T_q = 2.269) = 1.944 \pm 0.005$ for U_4 and 1.936 ± 0.005 for $\langle M^2 \rangle$.

The result for other T_q values has been shown in Fig. 3(c), which shows an interesting power-law behavior (the inset)

with the exponent $\gamma_{TT} = 0.49 \pm 0.01$ for $L = 1024$. Such a power-law behavior is also seen in Fig. 3(d). We see that $\chi(T, T_q)$ shows a power-law behavior with T for all considered T_q 's with a varying exponent $\gamma(T_q)$. This dependence is power-law with the second exponent $\beta = 0.38 \pm 0.01$ [in this figure $T_c(T_q)$ has been abbreviated to T_c^q].

More important are the geometrical exponents, which more directly classify 2D critical models. In Figs. 4(a) and 4(b) these geometrical exponents have been specified for $T_q = 2.269$. We see that $D_f(T = T_c(T_q = 2.269)) \equiv \gamma_{lr} = 1.408 \pm 0.002$ and $\gamma_{mr}(T = T_c(T_q = 2.269)) = 1.981 \pm 0.002$. These should be compared to the values for the regular critical 2D Ising model, $D_f = \frac{11}{8}$ and $\gamma_{mr} = \frac{187}{96}$, showing that the loops for the disordered Ising model becomes more compact and twisted. The exponents for the distribution functions are also [see Fig. 4(b) and their insets] $\tau_r(T = T_c(T_q = 2.269)) = 3.12 \pm 0.03$, $\tau_m(T = T_c(T_q = 2.269)) = 2.00 \pm 0.02$, and $\tau_l(T = T_c(T_q = 2.269)) = 2.45 \pm 0.02$. The results have been gathered in Table I. According to Ref. [46] the exponent of loop lengths τ_l of the critical Ising model is related to fractal dimension of the loops D_f and d (the Euclidean dimension of space) via $\tau_l = \frac{d}{D_f} + 1$. If we generalize this equation by $\tau_l = \frac{\bar{d}}{D_f} + 1$, which yields 2.4 ± 0.002 (noting that the effective dimension of the critical Ising model is $\bar{d} = \frac{187}{96}$ [45]), we see that this relation is consistent with our numerical result for τ_l . In Table I we have also shown the results of the critical Ising model on the triangular critical uncorrelated percolation lattice [17] and the regular square lattice [42]. We conclude that the critical properties of the model deviate considerably from that for the critical uncorrelated percolation lattice as well as the regular lattice.

B. Off critical T_q 's

The critical properties of the model have been obtained in the previous subsection. One may ask whether the scaling behaviors are seen in the off-critical region, where T_q is lower than the critical one and HSC is in the subcritical

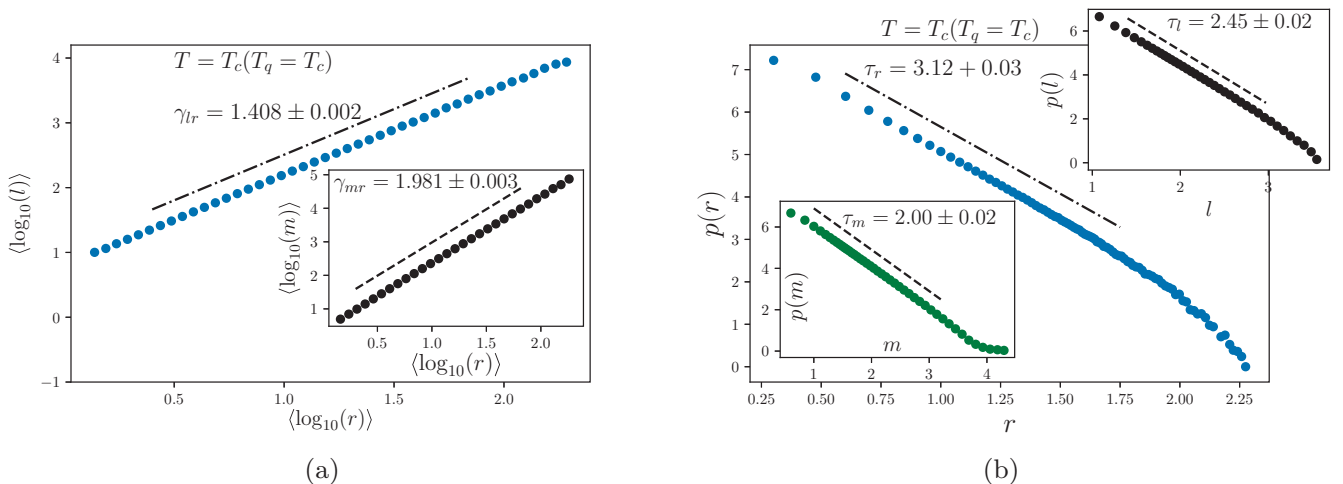


FIG. 4. (a) The fractal dimensions γ_{lr} and γ_{mr} , which are the slopes of the log-log plots. (b) The distribution functions of r , l , and m at $T = T_c(T_q = T_c)$.

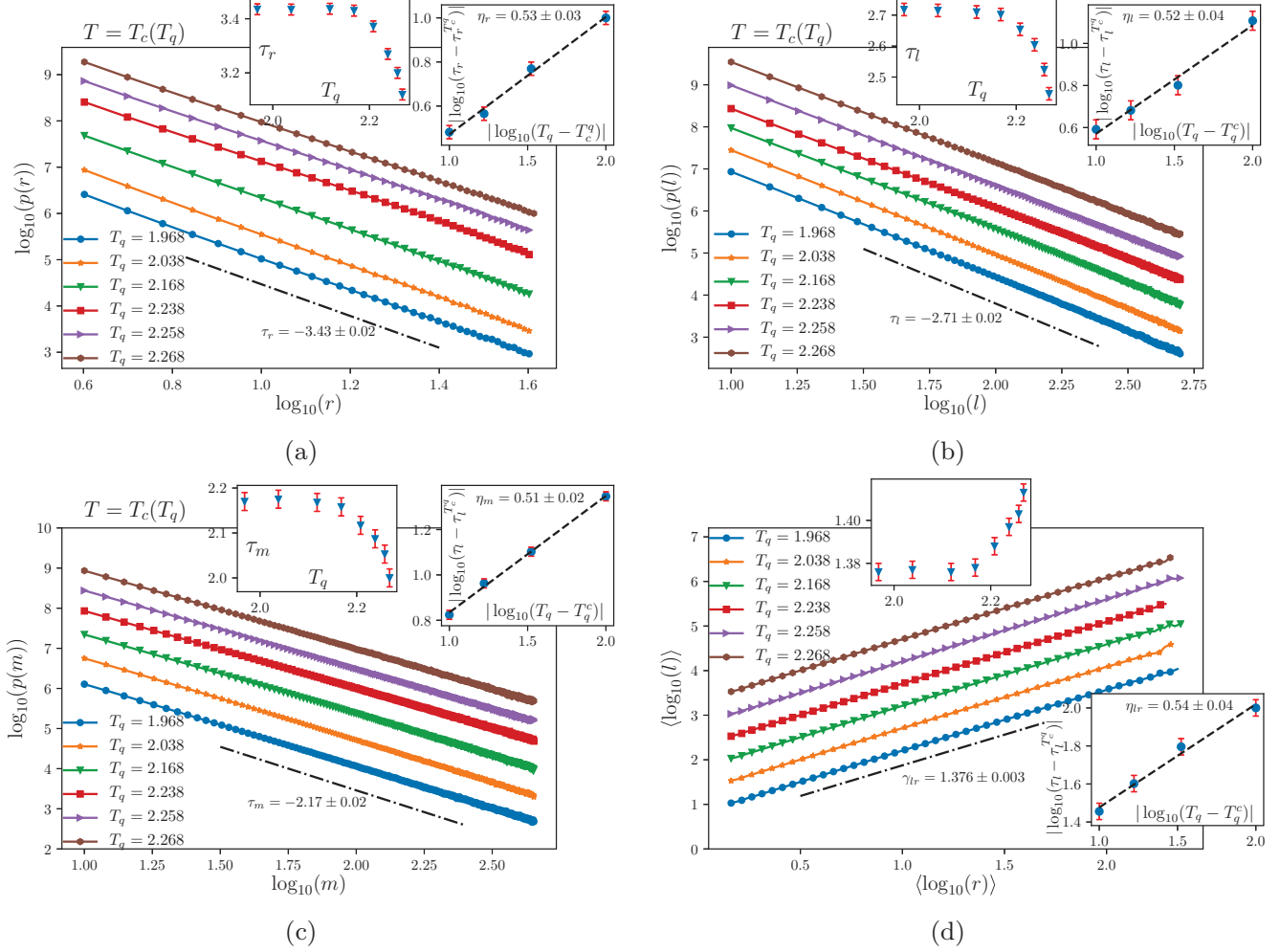


FIG. 5. Plot of the distribution function (a) gyration radius, (b) loop length, and (c) mass of the clusters in terms of T_q at the fixed dynamical temperatures $T = T_c(T_q)$ and $L = 1024$. Insets show the power-law behaviors with some well-defined exponents. (d) The fractal dimension in terms of T_q at the fixed dynamical temperatures $T = T_c(T_q)$ and $L = 1024$.

regime. For this we should examine the T_q 's which are close to the critical temperature and observe if they show scaling behavior or not. If the answer is positive, we can extract a secondary spectrum of the exponents [the first spectrum is for the dynamical temperatures in the vicinity of $T_c(T_q = 2.269)$, which were reported in the previous subsection]. Therefore in this subsection we vary T_q , and fix $T = T_c(T_q)$ (contrary to the previous subsection in which T_q was fixed to the critical value and the dynamical temperature was variant).

In Figs. 5(a)–5(c) we have examined this for the distribution function for the gyration radius, loop length, and cluster mass, respectively. In all cases we have seen the power-law behaviors with the exponents which run with T_q . At $T_q = 0$ one expects the results of ordinary Ising model, i.e., the fourth row of Table I, and for $T_q = T_c = 2.269$ we have reported the exponents in the previous section, i.e., the second row of Table I. For the other temperatures, we see from Figs. 5(a)–5(c) that the corresponding exponents are nearly constant for small T_q 's up to some point above which the exponents fall off rapidly towards the final value at $T_q = T_c$. More interestingly the graphs reveal that a power-law behavior arises in the close vicinity of $T_q = T_c$, in which the critical exponents scale

with $T_q - T_c$. The corresponding exponents are the secondary spectrum of the exponents that we have mentioned above.

The same features are seen for the fractal dimension D_f , i.e., Eq. (3) holds. The same equations also hold for τ_r , τ_l , and τ_m . Interestingly, all of the obtained exponents are more or less close to $\frac{1}{2}$ (note that the numerical accuracy may allow for different values). If we approximate these exponents by $\frac{1}{2}$, noting that the spin correlation length for the Ising model scales with T_q in the form $\zeta(T_q) \sim |T_q - T_c|^{-1}$, we conclude that all of the critical exponents vary linearly with $\frac{1}{\sqrt{\zeta(T_q)}}$. This phenomenon has also been seen in some previous works, e.g., the sandpiles [12], the Gaussian free field [36], the self-avoiding walk [14], and the loop-erased random walk [47] on the Ising-correlated percolation lattice.

IV. DISCUSSION AND CONCLUSION

In this paper we have considered the dynamical Ising model on the Ising-correlated square percolation lattice. The problem was motivated by the real porous media in which there are some correlations for the spatial configuration of the pores. We used the term *quenched Ising model* (QIM) for the

Ising model that is employed for controlling the correlations of the pores. For this model we also have used the phrase *artificial temperature* or *quenched temperature* (T_q), the quantity that tunes the correlations, and the population of pores. We have used four parallel methods to distinguish the presumable critical (dynamical) temperature for each quenched temperature.

We found that this system shows critical properties in the vicinity of some critical dynamical temperatures, with well-defined critical exponents and fractal dimensions. Up to our numerical observations, and within our numerical precision, these two transitions occur simultaneously in the case of study. This is in contrast to the case of an uncorrelated percolation lattice [17]. For $T_q = T_c^{2D \text{ square Ising}}$ we found that the critical dynamical temperature at the thermodynamic limit is $T_c = 1.94 \pm 0.002$. At this temperature the fractal dimension of the external perimeter of the connected spin clusters is $D_f(T = T_c(T_q = 2.269)) = 1.408 \pm 0.002$. The other exponents have been reported in Table I.

In the off-critical host spanning clusters (HSCs), however, we uncovered that there is a second spectrum of the critical exponents which are related to the off-criticality of the host media. In this case we varied T_q 's and fixed T 's to the critical values. We have seen that the first spectrum of exponents (D_f , τ_r , τ_l , τ_m , and β) scale with $T_q - T_c$ with other critical exponents. The absolute value of the exponents of the distribution functions of the geometrical statistical quantities increase under the decreasing of the correlation length of the random host network (with decreasing T_q). The lower the correlation length is, the sooner the distribution function of geometrical quantities will fall off, and the larger the absolute value of the corresponding exponents will be. The exponent for the fractal dimension is close to the fractional value $\frac{1}{2}$. Based on this result, and the results that were obtained for other models on the Ising-correlated percolation lattices, we propose that this $\frac{1}{2}$ (for the fractal dimension) is a super-universal quantity for the critical models on the Ising lattices.

-
- [1] A. R. Kose, B. Fischer, L. Mao, and H. Koser, *Proc. Natl. Acad. Sci. USA* **106**, 21478 (2009).
- [2] J. Philip, P. Shima, and B. Raj, *Appl. Phys. Lett.* **91**, 203108 (2007).
- [3] J. H. Kim, F. F. Fang, H. J. Choi, and Y. Seo, *Mater. Lett.* **62**, 2897 (2008).
- [4] H. Kikura, J. Matsushita, N. Kakuta, M. Aritomi, and Y. Kobayashi, *J. Mater. Process. Technol.* **181**, 93 (2007).
- [5] H. Kikura, J. Matsushita, M. Matsuzaki, Y. Kobayashi, and M. Aritomi, *Sci. Technol. Adv. Mater.* **5**, 703 (2004).
- [6] M. Matsuzaki, H. Kikura, J. Matsushita, M. Aritomi, and H. Akatsuka, *Sci. Technol. Adv. Mater.* **5**, 667 (2004).
- [7] J. J. Benkoski, S. E. Bowles, R. L. Jones, J. F. Douglas, J. Pyun, and A. Karim, *J. Polym. Sci. B* **46**, 2267 (2008).
- [8] D. Dhar, *J. Math. Phys.* **18**, 577 (1977).
- [9] D. Dhar, *J. Phys.* **49**, 397 (1988).
- [10] M. Najafi, M. Ghaedi, and S. Moghimi-Araghi, *Physica A* **445**, 102 (2016).
- [11] M. Najafi, *J. Phys. A* **49**, 335003 (2016).
- [12] J. Cheraghalizadeh, M. N. Najafi, H. Dashti-Naserabadi, and H. Mohammadzadeh, *Phys. Rev. E* **96**, 052127 (2017).
- [13] E. Daryaei and S. Rouhani, *Phys. Rev. E* **89**, 062101 (2014).
- [14] J. Cheraghalizadeh, M. Najafi, H. Mohammadzadeh, and A. Saber, *Phys. Rev. E* **97**, 042128 (2018).
- [15] M. Najafi, *J. Phys. A: Math. Theor.* **51**, 175001 (2018).
- [16] Y. Gefen, B. B. Mandelbrot, and A. Aharony, *Phys. Rev. Lett.* **45**, 855 (1980).
- [17] M. Najafi, *Phys. Lett. A* **380**, 370 (2016).
- [18] P. D. Scholten and M. Kaufman, *Phys. Rev. B* **56**, 59 (1997).
- [19] G. Burlak, *Commun. Math. Anal. Conf.* **3**, 42 (2011).
- [20] B. M. McCoy and T. T. Wu, *Phys. Rev.* **176**, 631 (1968).
- [21] R. Shankar and G. Murthy, *Phys. Rev. B* **35**, 3671 (1987).
- [22] B. Van der Hoeven, *Phys. Rev. Lett.* **20**, 719 (1968).
- [23] P. Handler, D. Mapother, and M. Rayl, *Phys. Rev. Lett.* **19**, 356 (1967).
- [24] V. S. Dotsenko and V. S. Dotsenko, *Adv. Phys.* **32**, 129 (1983).
- [25] A. W. W. Ludwig, *Phys. Rev. Lett.* **61**, 2388 (1988).
- [26] B. N. Shalaev, *Fiz. Tverd. Tela* **26**, 3002 (1984).
- [27] R. Shankar, *Phys. Rev. Lett.* **58**, 2466 (1987).
- [28] K. Ziegler, *J. Phys. A* **18**, L801 (1985).
- [29] K. Ziegler, *Nucl. Phys. B* **344**, 499 (1990).
- [30] K. Ziegler, *Europhys. Lett.* **14**, 415 (1991).
- [31] V. Andreichenko, V. S. Dotsenko, W. Selke, and J.-S. Wang, *Nucl. Phys. B* **344**, 531 (1990).
- [32] J.-S. Wang, W. Selke, V. S. Dotsenko, and V. Andreichenko, *Physica A* **164**, 221 (1990).
- [33] J.-K. Kim and A. Patrascioiu, *Phys. Rev. Lett.* **72**, 2785 (1994).
- [34] H. G. Ballesteros, L. A. Fernandez, V. Martin-Mayor, A. MunozSudupe, G. Parisi, and J. J. Ruiz-Lorenzo, *Phys. Rev. B* **58**, 2740 (1998).
- [35] J. Cheraghalizadeh, M. Najafi, and H. Mohammadzadeh, *J. Stat. Mech.* (2018) 083301.
- [36] J. Cheraghalizadeh, M. N. Najafi, and H. Mohammadzadeh, *Eur. Phys. J. B* **91**, 81 (2018).
- [37] S. Prakash, S. Havlin, M. Schwartz, and H. E. Stanley, *Phys. Rev. A* **46**, R1724 (1992).
- [38] A. Weinrib, *Phys. Rev. B* **29**, 387 (1984).
- [39] A. Coniglio, C. R. Nappi, F. Peruggi, and L. Russo, *J. Phys. A* **10**, 205 (1977).
- [40] A. Coniglio, H. E. Stanley, and W. Klein, *Phys. Rev. Lett.* **42**, 518 (1979).
- [41] E. Stoll and C. Domb, *J. Phys. A* **11**, L57 (1978).
- [42] M. Najafi, *J. Stat. Mech.: Theor. Exp.* (2015) P05009.
- [43] G. Delfino, *Nucl. Phys. B* **818**, 196 (2009).
- [44] J. Hoshen and R. Kopelman, *Phys. Rev. B* **14**, 3438 (1976).
- [45] B. Duplantier and H. Saleur, *Phys. Rev. Lett.* **63**, 2536 (1989).
- [46] W. Janke, T. Neuhaus, and A. M. Schakel, *Nucl. Phys. B* **829**, 573 (2010).
- [47] J. Cheraghalizadeh and M. Najafi, [arXiv:1807.04648](https://arxiv.org/abs/1807.04648).